CETRA2024 15-17 May 2024, Cavtat, Croatia
8th International Conferenceon Road and Rail Infrastructure

FINITE ELEMENT MODEL UPDATING OF CIVIL ENGINEERING STRUCTURES: SIGNIFICANCE OF MODE SHAPE PARING

Suzana Ereiz[1], Javier Fernando Jiménez-Alonso[2], Ivan Duvnjak[1], Marko Bartolac[1], Janko Košćak[1], Jurica Pajan[1]
[1] University of Zagreb, Faculty of Civil Engineering, Croatia
[2] Universidad de Sevilla, Escuela Superior de Ingeniería, Spain

Abstract

Finite element models are created to describe the behaviour of the structure and predict its response to the loads to which the structure is subjected. Due to the basic assumptions of the finite element method, the behaviour predicted by the numerical model deviates from the actual behaviour. With the aim of reducing this deviation, the developed numerical model is calibrated through the process of model updating. This process is usually based on dynamic parameters such as mode shapes and natural frequencies. In this way, the residuals of the natural frequencies and modal shapes are defined, and their magnitudes are optimised. For this purpose, the modal assurance criterion is most used for mode shapes. The aforementioned criterion is most sensitive to large differences and relatively insensitive to small differences in the mode shapes. For this reason, this paper compares the application of different criteria to compare the mode shapes with the results of the model update of the laboratory model of a pedestrian bridge.

Keywords: finite element model updating, mode shape paring, structural dynamic properties, Pareto optimal front

1 Introduction

Numerical modelling in civil engineering, often using the finite element method, simulates structural responses. However, due to different assumptions and predictions, the obtained model may not fully represent real structural behavior [1]. To address this, results from experimental investigations are utilized in the finite element model updating process, enhancing the correspondence between numerical models and actual structural behavior. Various methods, typically categorized as deterministic or stochastic [2], can be employed for this purpose. Practical engineering employs deterministic methods [3], formulating FEMU as an optimization problem characterized by bi-objective optimization and a decision-making subproblem. This results in a set of possible optimal solutions, known as the Pareto optimal front [4]. The decision-making subproblem involves selecting the best solution (knee point) from the elements of the Pareto optimal front.
The bi-objective optimization problem is typically defined through residuals, representing the difference between numerically predicted and experimentally obtained structural dynamic parameters. Natural frequency residuals are mainly expressed as relative differences, while there are various ways to define the difference in mode shapes [5]. Commonly, the modal assurance criterion and its derivations are employed for this purpose [6]. However, practical application reveals a drawback, with the criterion easily converging to high values,

even when the numerical model doesn't fully correspond to real structural behavior [7]. This leads to significant differences between natural frequency and mode shape residuals.
To address this, the paper analyses the impact of alternative mode shape residuals formulations, including Root Mean Square Error [8], Modal Scaling Factor [9], Mean Absolute Error [10], and Modal Assurance Criterion [11], on multi-objective FEMU results. FEMU with different mode shape comparison criteria is conducted on the laboratory footbridge. The criteria involve comparing the Pareto optimal front and the "knee point" position. The paper is structured as follows: the 2nd section presents the theoretical background of multi-objective FEMU optimization, the 3rd section introduces observed mode shape comparison criteria with equations, the 4th section describes the footbridge, initial numerical model, experimental investigation, and FEMU steps with different mode shape residuals. The 5th section discusses results, comparison, and validation, while the final 6th section provides concluding remarks.

2 Multi objective finite element model updating

Applying the maximum likelihood method, the FEMU problem becomes an optimization task, defining differences between numerical predictions and experimental results as residuals. For structural dynamic properties, natural frequencies residuals (r^f_t) are relative differences, and mode shape residuals (r^m_t) are commonly expressed through the modal assurance criterion and its derivatives. The general formulation of the multi-objective FEMU problem is as follows:

$$\min f(\theta) = (f_1(\theta)\ f_2(\theta)) = min\left(\sum_{t=1}^{m_f} r_t^f(\theta)^2 \quad \sum_{t=1}^{m_m} r_t^m(\theta)^2\right) \tag{1}$$

where $f(\theta)$ represent the multi objective function, $f_1(\theta)$ and $f_2(\theta)$ is the first and second multi objective function residuals, m_f and m_m are the natural frequency $r_t(\theta)$ and mode shape $r^j_t(\theta)$ residual vector size. To guarantee that two types of residuals are well-balanced, they may be normalized as:

$$r_t^f(\theta) = \frac{f_{num,t}(\theta) - f_{exp,t}}{f_{exp,t}} \quad t = 1, 2,.., m_f \tag{2}$$

$$r_t^m(\theta) = \sqrt{\left(\frac{\left(1-\sqrt{MAC_t(\theta)}\right)^2}{MAC_t(\theta)}\right)} \quad t = 1, 2,.., m_m \tag{3}$$

The residuals from the Eq.(3) commonly express mode shape discrepancies. Various formulations arise when different mode shape comparison criteria are applied. The next section elaborates on these different formulations for effective criterion comparison.

3 Mode shapes comparison criteria

For comparing mode shapes various methods such as the modal assurance criterion, root mean square error, mean square error, and modal scaling factor.

3.1 Modal assurance criterion - MAC

MAC, or mode shape correlation coefficient [11], quantifies the correspondence between a mode shape at a specific natural frequency (ϕ_t^{num}) and the reference mode shapes at the peak of the power spectral density function. It is computed as the normalized scalar product of two vector sets, ϕ_t^{exp} and ϕ_t^{num}, resulting in a MAC matrix that reveals the relationship between experimental, ϕ_t^{exp} and numerically, ϕ_t^{num} mode shapes.

$$MAC\left(\phi_t^{exp},\phi_t^{num}\right)=\frac{\left|\left\{\phi_t^{exp}\right\}^T\left\{\phi_t^{num}\right\}\right|^2}{\left|\left\{\phi_t^{num}\right\}^T\left\{\phi_t^{exp}\right\}\right|} \tag{4}$$

ranges from 0 to 1, with 1 signifying perfect mode shape correlation and 0 indicating no correlation between the two mode shapes.

3.2 Root mean square error - RMSE

RMSE is a quadratic validation rule that gauges the average error magnitude, calculated as the square root of the average squared difference between experimentally obtained and numerically predicted mode shapes.

$$RMSE_t=\sqrt{\frac{1}{K}\sum_{k=1}^{K}\left(\phi_{k,t}^{exp}-\phi_{k,t}^{num}\right)^2} \tag{5}$$

$$r_t^m\left(\theta\right)=\frac{RMSE_t}{\left(1-\sqrt{\left(RMSE_t\right)^2}\right)^2} \tag{6}$$

In the Eq. (5) t is the observed mode, $\phi_{k,t}^{\exp}$ is the experimentally obtained normalized mode shape at the k^{th} point, $\phi_{k,t}^{num}$ is the corre-sponding numerical result. K is the total number of observed points on the structures. RMSE ranges from 0 to ∞, establishing a direct relationship with MAC. A perfect mode shape correlation (MAC = 1) corresponds to RMSE = 0 [8].

3.3 Mean absolute error - MAE

MAE is the average of absolute differences between numerically predicted ($\phi_{k,t}^{num}$) and experimentally ($\phi_{k,t}^{\exp}$) mode shapes, assuming consistent meanings for all individual differences.

$$MAE_t=\frac{1}{K}\sum_{k=1}^{K}\left|\phi_{k,t}^{num}-\phi_{k,t}^{exp}\right| \tag{7}$$

$$r_t^m\left(\theta\right)=\frac{MAE_t}{\left(1-\sqrt{\left(MAE_t\right)^2}\right)^2} \tag{8}$$

For assessing the accuracy of continuous variables, MAE and RMSE are widely employed. Like RMSE, MAE ranges from 0 to ∞. Unlike MAE, RMSE emphasizes larger errors due to the squaring of errors before averaging [10].

3.4 Modal scaling factor - MSF

MSF normalizes two or more mode shapes for subsequent processing. If $\phi_t^{\exp}$ and ϕ_t^{num} represent the tth experimentally obtained and numerically predicted mode shapes and ($\phi_{k,t}^{\exp}$) and ($\phi_{k,t}^{num}$) their transpose form, the MSF can be defined as follow:

$$MSF\left(\phi_t^{exp},\phi_t^{num}\right)=\frac{\left|\phi_t^{exp}\right|^T\left|\phi_t^{num}\right|}{\left|\phi_t^{num}\right|^T\left|\phi_t^{num}\right|} \tag{9}$$

$$r_t^m\left(\theta\right)=\frac{\left(1-\sqrt{\left(MSF_t\right)^2}\right)^2}{MSF_t^2} \tag{10}$$

For a good correlated mode shapes $\left(\phi_t^{exp}=\phi_t^{num}\right)$, $MSF\left(\phi_t^{exp},\phi_t^{num}\right)=MSF\left(\phi_t^{num},\phi_t^{exp}\right)=1$ while for $\phi_t^{exp}=a\phi_t^{num}$, $MSF\left(\phi_t^{exp},\phi_t^{num}\right)=a$ and $MSF\left(\phi_t^{num},\phi_t^{exp}\right)=1/a$.

4 FEMU of the laboratory footbridge

4.1 Description of the structure

The laboratory footbridge (Figure 1) is a simply supported structure with a 9.7 m single span (total length 10 m) and a 1.5 m width, constructed using FRP GFRP profiles and carbon FRP (CFRP) strips. It features panels mounted on three stringers with lateral displacements constrained by transverse beams. GFRP stringers consist of an I-profile and two U-profiles spaced 0.75 m apart, with GFRP elements serving as lateral restraints every 1.25 m from supports and every 1.20 m along the entire length. CFRP strips, attached with epoxy adhesive, enhance bending stiffness along the stringers. The handrails consist of stainless-steel cables crossing GFRP SHS profiles, connected to U profiles with bolts. Concrete blocks at both ends prevent damage and facilitate pin and roller support installation. GFRP L profiles and steel bolts assemble the bridge structure, and joints are achieved with bolts and 8-mm diameter clamps.

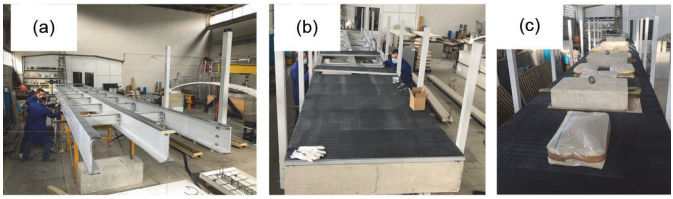

Figure 1 Ultra - lightweight FRP laboratory footbridge a) assembling of super-structure b) bridge walking surface c) ambient vibration test

4.2 Initial numerical model

The FRP bridge's initial numerical model (FEM) was created using Ansys on a PC with a 3.59 Hz processor and 16 GB RAM. The mesh comprises 28,293 elements, utilizing SHELL 181, 3D linear beam elements (BEAM 188), 3D solid elements (SOLID185), and COMBIN 14 elements for support modelling in both longitudinal and transversal directions.

Material characteristics of steel E_s = 210 GPa and concrete E_c = 35 GPa components are assigned. The GFRP profiles have the modulus of elasticity in x direction = 24 GPa, and in y direction = 7 GPa. The GFRP deck panels have the modulus = 20.5 GPa x direction, and = 8 GPa in y direction. The material density = 1800 was assigned to GFRP elements. The CFRP strips have the modulus of elasticity = 139 GPa, material density = 1550 kg/m^3. Assigned a Poisson ratio (v = 0.23) to all elements, modal analysis was conducted to obtain numerical natural frequencies and mode shapes for each mode (Figure 2).

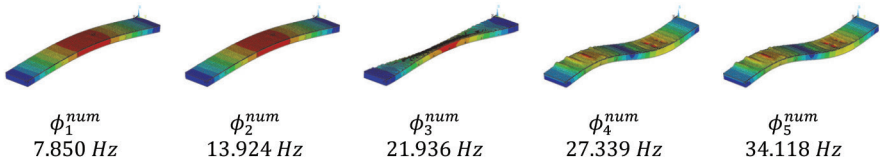

Figure 2 Natural frequencies and mode shapes obtained from the initial FEM

4.3 Experimental investigation of the structure

4.3.1 Static test

The static test involved using twenty sandbags (300 kg) and four concrete blocks (760 kg) on the structure's middle to measure deflection (Figure 1.c). The total mass was distributed over the deck for a uniform load of 0.7 kN/m^2, resulting in a maximum deflection of 12.8 mm at the span's midpoint12.8 mm.

4.3.2 Dynamic test

The dynamic properties of the laboratory footbridge were experimentally identified through Operational Modal Analysis (OMA) during ambiental excitation (Figure 3.). The 18 sensors were arranged in two lines with 9 measuring points in each in the vertical direction in order to collect and analyse data on acceleration to obtain data on torsional shapes. Based on the collected data mode shapes and corresponding natural frequencies are determined. For detailed description of the performed experimental investigation, the readers are referred to [12].

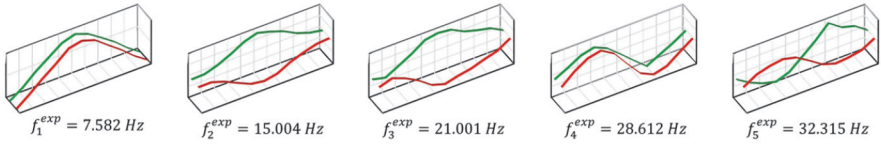

Figure 3 Experimental identification during ambient vibration a) measuring point arrangement, b) characteristic mode shape for corresponding natural frequencies

4.4 Experimental investigation of the structure

To assess accuracy of the initial FEM performance, a comparative analysis was performed based on the difference between the natural frequencies and MAC for mode shapes. The results of the analysis are shown in the Table 1.

Table 1 Comparison structural behaviour predicted by numerical model and experimentally obtained using absolute difference of the natural frequency values (Δf_t) and different mode shape comparison criterion

Mode t	f_t^{num} [Hz]	f_t^{exp} [Hz]	Δf_t [%]	MAC [/]	MAE [/]	RMSE [/]	MSF [/]
1	7.86	7.58	3.60	0.999	0.019	0.024	1.025
2	13.93	15.00	7.20	0.986	0.082	0.094	1.110
3	21.94	21.00	4.45	0.929	0.136	0.167	0.958
4	27.34	28.61	4.45	0.978	0.093	0.114	1.064
5	34.12	32.32	5.58	0.915	0.197	0.243	1.269

The most relevant updating parameters were selected using the sensitivity analysis. Based on the performed analysis results, eight updating parameters were selected. Those include $E_{1,GFRP,P}$ (θ_1) and $E_{2,GFRP,P}$ (θ_2), $E_{1,GFRP,D}$ (θ_3) and $E_{2,GFRP,D}$ (θ_4), $E_{1,CFRP,S}$ (θ_5), $E_{2,CFRP,S}$ (θ_6), E_S(θ_7 - θ_9), stiffness of longitudinal, k_{lon} (θ_{10}), and transversal k_{tran} (θ_{11}) spring boundary conditions. The vector of the initial values of the updating parameters was set θ = [24 GPa, 7 GPa, 20.5 GPa, 8 GPa, 139 GPa, 34.5 GPa, 200 GPa, 200 GPa, 200 GPa, $1 \cdot 10^8$ N/m, $1.5 \cdot 10^8$ N/m].

4.5 Solution of the MO FEMU problem using different formulation of the mode shape residuals

Using various formulations of mode shape residuals, MU FEMU optimizes the FEM with the Harmony Search algorithm [13]. The optimization process is conducted with established parameters: (i) population size PS = 100; (ii) maximum number of iterations = 50; (iii) objective function tolerance ;(iv) new population size; (v) harmony memory pitch adjustment and (vi) pitch adjusting rate. The position of the knee point results in the numerical model with the natural frequency and mode shape residual shown in the Table 2.

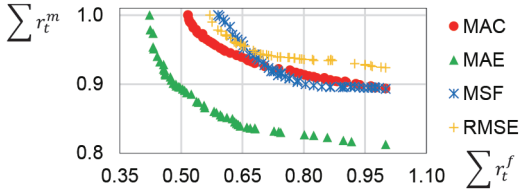

Figure 4 Comparison of the normalized Pareto optimal front obtained based on the different formulations of the mode shape residuals

Table 2 Comparison of the optimal numerical model obtained by FEMU using different mode shape criterion

	Mode, t	1	2	3	4	5
MAC		7.45	15.03	20.71	28.25	31.93
	[%]	-1.74	0.15	-1.40	-1.27	-1.18
	MAC [-]	0.999	0.986	0.929	0.979	0.915
MAE		7.68	15.02	20.99	28.92	32.16
	[%]	1.29	0.11	-0.05	1.08	-0.47
	MAE [-]	0.001	0.027	0.119	0.034	0.146
MSF		7.46	15.04	20.72	28.29	31.95
	[%]	-1.61	0.24	-1.34	-1.13	-1.13
	MSF [-]	1.024	1.109	1.044	1.063	1.274
RMSE		7.49	14.85	20.71	27.89	21.94
	[%]	1.21	1.03	1.39	2.52	1.16
	RMSE [-]	0.026	0.094	0.168	0.112	0.245

5 Validation and discussion of the results

Observing the natural frequency values in Table 2. for updated numerical models with various mode shape comparison criteria, MAE yields the lowest sum of absolute errors (Δf_t). Further comparison involves numerically demonstrating the static test performed experimentally, with deflection values presented in Table 3. for models updated using different criteria.

Table 3 Comparing the mid-span deflection from four optimal numerical models

Numerical model	**Deflection** [mm]	
	Numerical	**Experimental**
MAC	12.96	12.80
MAE	12.72	
MSF	12.95	
RMSE	13.01	

Results show variations in solutions (0.63% to 1.64%) due to different mode shape comparison criteria influencing the numerical model update. Notably, the MAE criteria yield the best match, aligning the numerical model's deflection in the span's middle closely with the experimentally determined value.

6 Conclusion

This paper evaluates various mode shape comparison criteria (MAC, MAE, MSF, and RMSE) for updating a numerical model of a benchmark structure (laboratory footbridge). Performance is compared to static test results, revealing that employing different mode shape criteria in FEMU leads to distinct optimal numerical models. The MAE criterion stands out, yielding a model with the lowest sum of observed natural frequencies error compared to MAC, MSF, and RMSE.

Notably, the MAE-based updated model aligns best with experimentally obtained results in static performance. In summary, the MAE criterion excels in addressing the multi-objective FEMU problem for civil engineering structures, warranting further investigation into dynamic response comparisons.

References

[1] Ereiz, S., Duvnjak, I., Jiménez, J.F.A.: Review of finite element model updating methods for structural applications, Structures, 41 (2022) 1, pp. 684–723, DOI: 10.1016/j.istruc.2022.05.041

[2] Marwala, T.: Finite-element-model updating using computational intelligence techniques: Applications to structural dynamics, 1st edition, London, England, Springer, 2010.

[4] Cuate, O., Schütze, O.: Pareto explorer for finding the knee for many objective optimization problems, Mathematics, 8 (2020) 10, DOI: 10.3390/math8101651

[5] Ewins, D.J.: Model validation: Correlation for updating, Sādhanā, 25 (2000), pp. 221-234

[6] Sehgal, S., Kumar H.: Structural Dynamic Model Updating Techniques: A State of the Art Review, Archives of Computational Methods in Engineering, 23 (2015), pp. 515–533

[7] Pastor, M., Binda, M., Harčarik, T.: Modal assurance criterion, Procedia Engineering, 48 (2012), pp. 543–548

[8] Bakhshizade, A., Reza Ashory, M.: Root mean square error criterion using operational deflection shape curvature for structural damage detection, Mathematical modelling in Engineering, 2 (2015), pp. 96-101

[9] Allemang, R.J., Brown, D.L.: Correlation Coefficient for Modal Vector Analysis, International Modal Analysis Conference & Exhibit, pp. 110-116, Orlando, Florida, 8-10 November 1982.

[10] Gupta, A.K.: Response Spectrum Method in seismic analysis and design of structures, Bulletin of the New Zealand Society for Earthquake Engineering, 26 (1993) 3, DOI: 10.5459/bnzsee.26.3.369

[11] Allemang, R.J.: The modal assurance criterion - Twenty years of use and abuse, Journal of Sound and Vibration, 37 (2003) 8, pp.14–21

[12] Gallegos-Calderón, C., Naranjo-Pérez, J., Díaz, I.M., Goicolea, J.M.: Identification of a human-structure interaction model on an ultra-lightweight FRP footbridge, Applied Sciences (Switzerland), 11 (2021) 14, DOI: 10.3390/app11146654

[13] Jiménez-Alonso, J.F., Naranjo-Perez, J., Pavic, A., Sáez, A.: Maximum Likelihood Finite-Element Model Updating of Civil Engineering Structures Using Nature-Inspired Computational Algorithms, Structural Engineering International, 31 (2020) 2, DOI: 10.1080/10168664.2020.1768812